Interface-phonon dispersion and confined-optical-mode selection rules of GaAs/AlAs superlattices studied by micro-Raman spectroscopy

R. Hessmer,* A. Huber,† T. Egeler, M. Haines, G. Tränkle, G. Weimann, and G. Abstreiter
Walter Schottky Institut, Technische Universität München, D-8046 Garching, Germany
(Received 30 January 1992)

Using micro-Raman spectroscopy, we study backscattering from (010) and ($1\bar{1}0$) surfaces of [001]-grown superlattices and establish experimental selection rules. By changing the momentum transfer $q_\parallel$ parallel to the superlattice layers over a wide range ($0 \le q_\parallel \le 9\times10^5$ cm^{-1}), we studied the dispersion of the interface phonons. The measured dispersion curves are compared to calculations based on the dielectric-continuum model.

I. INTRODUCTION

The optical phonons of GaAs/AlAs [001]-oriented superlattices (SL's) have attracted considerable interest since their early observation.[1] The present state of understanding is reviewed in several recent articles.[2–6] The confined optical modes in the GaAs layers could be measured up to high order[7–9] and the corresponding frequencies are close to the appropriately folded phonon dispersion of bulk GaAs known from neutron-diffraction experiments.[10] For the confined modes in the AlAs layers a considerably smaller energetic spacing is expected from calculations of the phonon dispersion in bulk AlAs.[11,12] It is therefore difficult to resolve the signals of the various order confined modes of AlAs layers even when they are only some monolayers thick. Recent experimental results for a superlattice consisting of GaAs and AlAs layers of six monolayers each can be found in Ref. 9.

The vast majority of Raman measurements have concentrated on backscattering geometries from the (001) surface. The selection rules in this case did not attract much attention, probably due to the fact that LO modes are allowed and TO forbidden in these geometries for both the superlattice and the bulk. However strong deviations from bulklike selection rules were observed by Zucker *et al.*[13] in a special waveguiding structure which allowed a 90°-scattering geometry to be measured. Namely, LO modes were observed where TO modes were expected and vice versa. An explanation using the momentum associated with the phonon quantization was later given.[3] As the momentum of the mth-order quantized phonons, given by $m\pi/d$, where d is the corresponding layer width, was much larger than the momentum transfer q of the photon, it was proposed that the latter should be replaced by the former when deciding whether the optic mode has longitudinal transverse character. A recent microscopic calculation by Huang, Zhu, and Tang[14] agrees with these results.

Besides the confined optical modes and their selection rules, the interface (IF) phonons have been intensively studies.[1,15–17] These modes have atomic displacements which peak at the interfaces and rapidly decay into the GaAs and AlAs layers. Their frequencies lie between those of the bulklike TO and LO frequencies and exhibit a strongly anisotropic dispersion. Early evidence of such modes was observed at resonance in a GaAs/AlAs superlattice by Merlin *et al.*[1] Similar structures were later seen in more detail and clearly interpreted as the signals of interface phonons by Sood *et al.*[15] It is noted that both experiments were carried out in a backscattering geometry from the (001) surface where such modes should have energies close to the bulklike TO and LO energies in a perfect crystal. Their observation between the TO and LO frequencies was thus attributed to impurity-induced scattering under resonance conditions which gives access to a range of finite in-plane wave vectors $q_\parallel$. Also from the (001) surface not deviating from a perfect backscattering configuration, Nakayama, Ishida, and Samo[16] investigated a special air/GaAs/AlAsGaAs heterostructure. With this structure they were able to measure the dispersion of the two interface-phonon polariton modes in the AlAs frequency region even with the small in-plane moment obtainable under off resonance. Recently micro-Raman-spectroscopy results showing the dispersion of the IF phonons in GaAs/AlAs superlattices were presented.[17]

In this paper we present more detailed micro-Raman measurements of the dispersion of IF phonons together with measurements of TO and LO phonons in a number of unusual backscattering geometries with the laser in [$1\bar{1}0$] and [010] directions, perpendicular to ($1\bar{1}0$) cleavage and (010) polished planes. The small laser spot sizes at the sample surface (diameter < 1 μm) obtained by our microscope setup allows such configurations to be measured. We excite the IF phonons off resonance, and hence momentum is conserved. In other words, the momentum of the scattered phonon is fully defined by the laser energy together with the scattering geometry. By polishing and tilting the planes under different angles, the in-plane momenta $q_\parallel$ is varied over a wide range ($0 \le q_\parallel \le 9\times10^5$ cm^{-1}), enabling us to map out directly the interface-phonon dispersion.

II. EXPERIMENTAL DETAILS

Five different SL samples were used for the measurements. They were grown on [001] GaAs substrates by molecular-beam epitaxy. Figure 1(a) schematically shows a sample and some important axes, the labeling of which refers to the cubic conventional unit cell of the bulk materials where the cleavage planes are perpendicular to the [110] and [1$\bar{1}$0] axes, denoted $\tilde{x}$ and $\tilde{y}$, respectively. A second coordinate system consisting of the axes $\hat{\mathbf{x}}\|[100]$, $\hat{\mathbf{y}}\|[010]$, and $\hat{\mathbf{x}}$ is also shown. For backscattering from the (010) plane, the samples were polished perpendicular to the y axis.

The thickness of the GaAs layers d_1 is about 100 Å in all samples, whereas the thickness of the AlAs layers d_2 varies from 25 to 200 Å. These values, as determined by transmission electron microscopy, are given in Table I together with the number of periods and the resulting total SL thickness for the five samples studied.

The Raman spectra were obtained at temperature using a triple grating Dilor XY spectrometer with a focal length of 0.5 m. Excitation was achieved with the 568.2-nm (2.182-eV) or 530.9-nm (2.336-eV) lines of a Kr^+ laser. A microscope objective focuses the laser light onto the sample surface, and the same objective collects the signal. The spectrometer was used in the subtractive mode with a spectral resolution of 3.0 cm^{-1} at 568.2 nm and 3.5 cm^{-1} at 530.9 nm. The signal was amplified by a multichannel plate and detected by a cooled Si diode array.

As already mentioned, different values of $q_{\|}$ can be achieved by tilting and polishing the samples under different angles. Figure 1(b) shows a typical scattering geometry. The sample is polished at an angle of β with respect to the layer normal and tilted so that the SL layers are oriented at an angle of γ with respect to the direction of the incident laser light. We study samples with $\beta=0°$ and $\beta=30°$ and measure for various tilt angles γ. The angle of polishing β and tilt angle γ determine the angle of incidence θ for the laser light. From the figure it can be seen that $\theta=\gamma-\beta$. Because of refraction, the corresponding angle inside the sample reduces to θ_1 given by $\sin\theta=n\sin\theta_1$, where n is the refractive index of the SL. The refractive index n of the SL was weighted by the individual layer thickness

$$n=(n_1d_1+n_2d_2)/(d_1+d_2)\ ,$$

with values for n_1 (GaAs) and n_2 (AlAs) taken from Refs. 18 and 19. The phonon momentum q is given by $q=4\pi n/\lambda$, where λ is the wavelength of the incident laser light. In the figure, q, together with its components

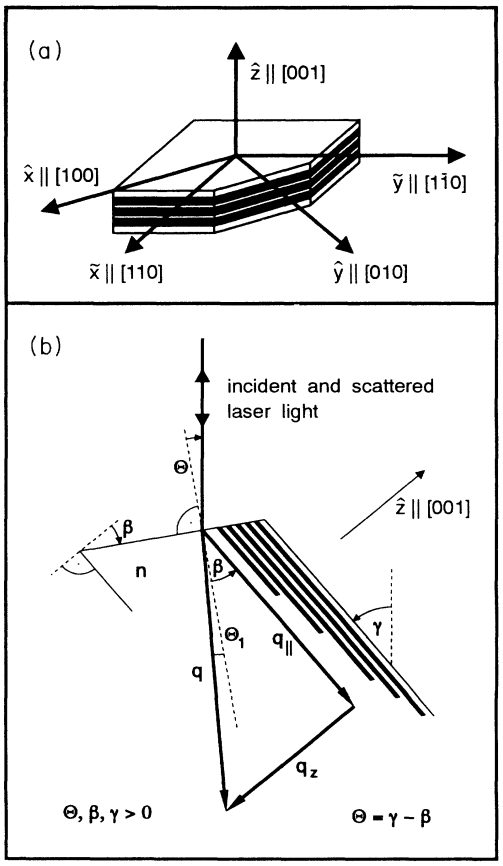

FIG. 1. (a) Schematic of a superlattice grown along [001] (the z direction). The axes $\hat{\mathbf{x}}\|[110]$ and $\hat{\mathbf{y}}\|[1\bar{1}0]$ are perpendicular to cleavage planes. Some samples were polished perpendicular to the [010] axis (the y direction), as indicated in the figure. (b) The phonon wave vector $\mathbf{q}$ and its components parallel $\mathbf{q}_{\|}$ and perpendicular $\mathbf{q}_z$ to the SL layers for a sample tilted and polished by the angles γ and β, respectively. The laser light is oriented at an angle θ (θ_1) outside (inside) the sample with respect to the surface normal.

$q_{\|}$ and q_z parallel and perpendicular to the layers, are indicated by the corresponding arrows. They are related by

$$q_{\|}=q\cos(\beta+\theta_1)\ , \tag{1}$$

$$q_z=q\sin(\beta+\theta_1)\ . \tag{2}$$

It is noted that due to the relatively large aperture of the microscope objective, backscattered laser light over a range of scattering angles is collected. This leads to an envelope of detected $q_{\|}$ and q_z values. However, the large refractive index difference between air and the SL

TABLE I. The structure parameters of the samples.

Sample	*A*	*B*	*C*	*D*	*E*
d_1 (Å)	105	95	105	105	100
d_2 (Å)	25	45	75	135	200
Number of periods	90	60	50	50	50
Total SL thickness in the [001] direction (μm)	1.17	0.84	0.9	1.2	1.5

(refractive index of about 3.5) helps to reduce this effect. For instance, a typical variation in collected θ of 30° leads to only a 8.2° variation in θ_1.

III. RESULTS AND DISCUSSION

Various measurements from the (010) polished (Fig. 2) and (1$\bar{1}$0) cleaved (Fig. 3) surfaces are now discussed. The Raman spectra shown are obtained from sample *C* with the laser at 530.9 nm (2.336 eV) but are typical of what was observed. Phonons near the LO and TO frequencies are seen, along with interface modes lying in between. We note that due to the relatively thick layers, quantization effects of the optic modes are not resolved. However, the relation for the quantized phonon wave vector, $m\pi/d > q$ still holds since $\pi/d = 3.14\times10^6$ cm^{-1} for the GaAs layers and $q = 8.94\times10^5$ cm^{-1}. The optical-mode selection rules predicted by the two methods described in the Introduction (which agree with each other for the shown geometries), together with the selection rules for bulk material, are written alongside the relevant spectrum in Figs. 2 and 3 and are now compared with the observed spectra. In Fig. 2 the $y(x,x)\bar{y}$ spectrum and in Fig. 3 the two depolarized spectra are in good agreement with the theoretical predictions. The $y(x,z)\bar{y}$, $y(z,x)\bar{y}$, and $\tilde{y}(\tilde{x},\tilde{x})\bar{\tilde{y}}$ spectra, however, are in conflict with the superlattice selection rules. In these three cases the observations could be explained if we assume that a significant part of the signal originates from the neighboring GaAs. However, this is unlikely due to the submicrometer laser spot which we carefully centered on the SL (using a piezodriven plate with a precision of 0.1 μm) by optimizing upon the IF phonon signal. Finally, the disagreement seen in the $y(z,z)\bar{y}$ and $\tilde{y}(z,z)\bar{\tilde{y}}$ traces are not explicable through invoking such a bulk contribution. Here, strong TO modes are observed for both GaAs and AlAs which are forbidden in both bulk and superlattice. It is clear that the microscopic theory[14] does not give an adequate description of our observations.

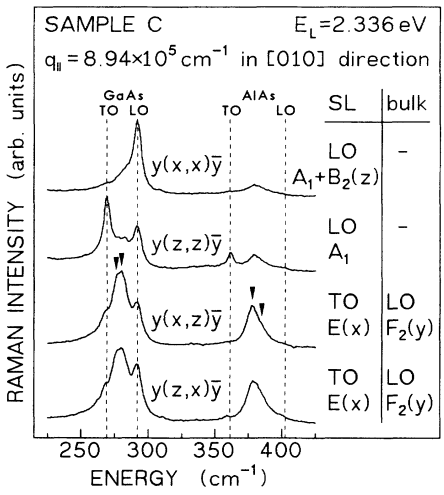

FIG. 2. Raman spectra of sample *C* at a laser wavelength of 530.9 nm ($E_L = 2.336$ eV). The four possible scattering configurations for backscattering from the (010) plane are shown. The dashed lines indicate the bulklike TO and LO frequencies; the arrows mark IF phonons. Alongside each spectrum, the predicted Raman scattering for optical phonon modes together with the corresponding Raman tensors (taken from Ref. 30) for the SL (point group D_{2d}) and bulk (point group T_d) are listed.

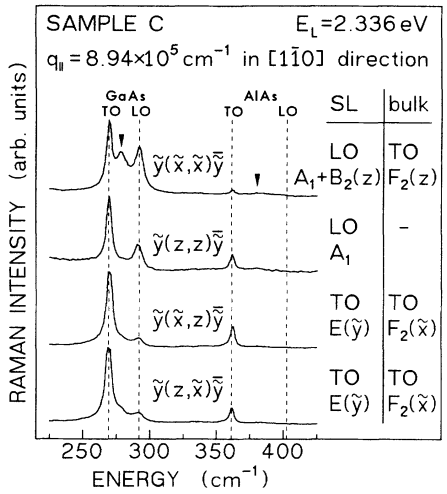

FIG. 3. The corresponding spectra to Fig. 2 but now with the wave-vector component $\mathbf{q}_\parallel$ in the $\tilde{y}$ direction, i.e., for backscattering from the (1$\bar{1}$0) plane.

Between the frequencies of the bulklike TO and LO phonons of GaAs and AlAs, respectively, additional peaks can be seen in Figs. 2 and 3 (marked by arrows) which are attributed to interface phonons. To determine the dispersion of these IF phonons, we measured their frequencies in different geometries, as shown explicitly in Fig. 4. The spectra are taken in crossed polarizations as these showed the most intense IF phonon signals. To de-

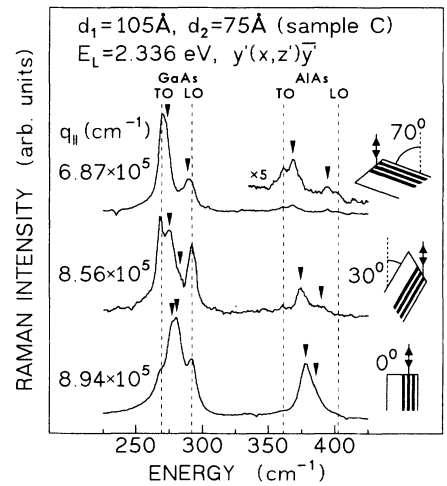

FIG. 4. Raman spectra in crossed polarization of sample *C* for different values of the wave-vector component $\mathbf{q}_\parallel$ parallel to the SL but with constant total momentum transfer $q = 8.94\times10^5$ cm^{-1}. Arrows mark the IF phonons. The corresponding scattering geometries are shown inset.

scribe the scattering geometries used, a new coordinate system is introduced. The system x,y',z' is the system x,y,z rotated about the x axis so that the y' axis is kept parallel to the incident laser light inside the sample. For geometries with the incident laser light in the (110) plane, an analogous system $\tilde{x},\tilde{y}',\tilde{z}'$ which emerges from the system $\tilde{x},\tilde{y},z$ is later used. In backscattering from a (001) surface, i.e., vanishing momentum transfer $q_\parallel$ parallel to the layers, the frequencies of the IF phonons are close to the frequencies of the confined TO and LO phonons and are no longer resolved (not shown in Fig. 4). With increasing $q_\parallel$, the frequencies of the IF phonons shift away from the TO and LO frequencies of GaAs and AlAs, respectively. The intensity of the IF phonons in the parallel configurations $y'(x,x)\bar{y}'$ and $y'(z',z',)\bar{y}'$ is much weaker than in the corresponding crossed polarizations shown. A comparable intensity of the IF phonons is only observed in the configuration $\tilde{y}'(\tilde{x},\tilde{x})\bar{\tilde{y}}'$. We also note that no change of the IF phonon frequencies could be measured between configurations with the laser light in the (y,z) plane or the $(\tilde{y},z)$ plane.

We now compare the measured IF phonon frequencies with the values calculated in the dielectric-continuum model. In this model the layers of the polar materials GaAs and AlAs are described by their dielectric functions $\epsilon_1(\omega)$ and $\epsilon_2(\omega)$ depending on the frequency ω but independent of the wave vector q. One can write $\epsilon(\omega)$ as

$$\epsilon(\omega)=\epsilon_\infty\frac{\omega^2-\omega_{\mathrm{LO}}^2}{\omega^2-\omega_{\mathrm{TO}}^2}\ , \tag{3}$$

where ϵ_∞ represents the high-frequency dielectric constant and $\omega_{\mathrm{TO}},\omega_{\mathrm{LO}}$ are the frequencies of the TO and LO phonons in the long-wavelength limit. The periodic structure of the SL is then incorporated by the periodic modulation of the dielectric function. Using Maxwell's equation $\nabla(\epsilon E)=0$, an implicit equation for the dispersion of IF phonons is obtained:[21]

$$\cos(q_zL)=\cosh(q_\parallel d_1)\cosh(q_\parallel d_2)+\kappa\sinh(q_\parallel d_1)\sinh(q_\parallel d_2)\ , \tag{4}$$

with

$$\kappa=\tfrac{1}{2}(\epsilon_1/\epsilon_2+\epsilon_2/\epsilon_1)\ ,$$

where $L=d_1+d_2$ is the SL period, the values of q_z and $q_\parallel$ are defined by Eqs. (1) and (2), and values for ϵ_∞ in GaAs and AlAs were taken from Ref. 22.

In Fig. 5 the peak positions of the IF phonons for the same sample as in Fig. 4 are shown for a range of $q_\parallel$, but in each case with the same total $q=8.94\times10^5$ cm^{-1}. They are plotted as a function of the dimensionless number $q_\parallel L$. The peak positions in a given spectrum were obtained by fitting Lorentzians to the trace. In different spectra for the same experimental conditions, the positions differ by about 3 cm^{-1}. Since no systematic difference of the peak positions obtained in the $y'(x,z')\bar{y}'$ and $\tilde{y}'(\tilde{x},\tilde{x})\bar{\tilde{y}}'$ configurations could be measured, values from various spectra for both configurations are averaged for each plotted $q_\parallel L$ value and shown in the figure.

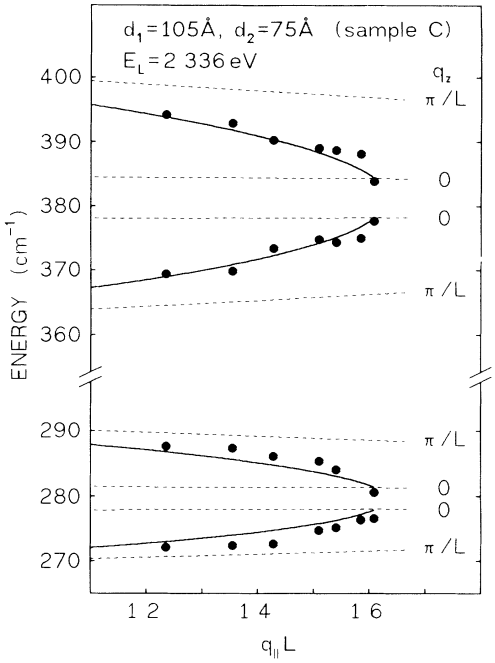

FIG. 5. Measured IF phonon energies (dots) and calculated dispersion curves (solid lines) for sample C as a function of the in-plane momentum transfer multiplied by the SL period $q_\parallel L$ where $L=105+75$ Å. The value of q_z is given by $q_z^2=q^2-q_\parallel^2$ with $q=8.94\times10^5$ cm^{-1}. The dashed lines show the limiting cases $q_z=0$ and $q_z=\pi/L$.

The solid lines in Fig. 5 are the calculated IF phonon-dispersion branches for q_z and $q_\parallel$ as defined by the experiment. The extreme limits for the solution of Eq. (4), namely, the IF phonon branches for $q_z=0$ and $q_z=\pi/L$, are shown by the dotted lines. It is seen that the resultant forbidden energy gap between the two IF mode branches is, within experimental error, not encroached upon even at large $q_\parallel L$ in agreement with the theory. Similar dispersion curves were obtained for the other samples.

For a comparison of the five samples with almost constant GaAs layer width but different thicknesses of the AlAs layers, we show in Fig. 6 the spectra of each sample in the same scattering geometry $\tilde{y}'(\tilde{x},\tilde{x})\bar{\tilde{y}}'$. The laser wavelength is 568.2 nm (2.182 eV). The observed IF phonon modes are marked by arrows. With increasing AlAs layer width, the intensity of the high-energy IF phonon in the AlAs region becomes larger. An opposite trend can be seen in the GaAs region. The asymmetry of the IF modes in the AlAs region was also observed by Sood *et al.*[15] and is attributed to the differing symmetry of the corresponding modes. That is, the symmetries of the modes in the GaAs region are simply opposite to those in the AlAs region, which explains the difference between the GaAs and AlAs IF phonon intensities observed in single spectra. As the symmetry flips when going through $d_1=d_2$, the symmetries of the IF phonons should also. This trend is seen in our results by the evo-

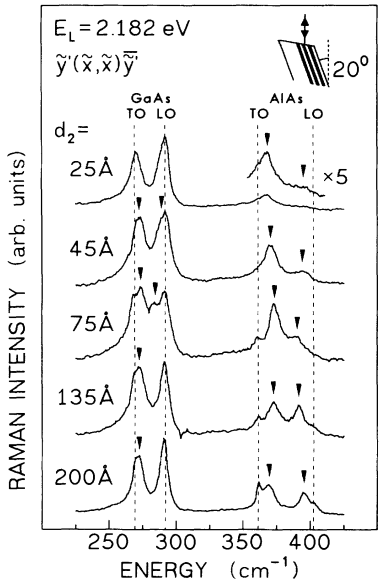

FIG. 6. Raman spectra of all samples in the scattering configuration $\tilde{y}'(\tilde{x},\tilde{x})\tilde{y}'$ at a laser wavelength of 568.2 nm ($E_L = 2.182$ eV) showing the changes in the IF mode energies and intensities for various ratios of d_1/d_2. Interface modes are marked by arrows.

lution of the intensity ratios of the interface modes as the AlAs layers "become thicker."

As a final demonstration that the IF phonons are well described by the dielectric-continuum model and also that phonon momentum is well defined, i.e., broadening of the signal due to impurity-induced scattering is not important, we measured the IF phonon dispersion as a function of the thickness ratio d_1/d_2. In Fig. 7 we show the experimental AlAs-like IF phonon energies (dots) for our set of samples, which have near constant d_1 and widely differing d_2 values, for three different geometries. The measured energies are compared with the calculated dispersion branches (solid lines). In order to be able to compare the different samples, we used for the calculations a GaAs layer width of $d_1 = 100$ Å. It is noted that in spite of the same laser energy in each geometry, q and $q_\parallel$ are not strictly constant with respect to d_1/d_2 due to the refractive index of the SL, which depends on the layer thicknesses. The effect is included in the calculations but is only small. Also shown (dotted lines) are the calculations for the two extreme geometries, $q_z = 0$ and $q_z = q$.

In each graph we observe the minimum in the energy difference of the two AlAs IF modes around $d_1 = d_2$ predicted by theory. Quantitatively good agreement between the measured and calculated energies is also found, except for sample E ($d_1/d_2 = 0.5$), which consistently shows values closer to the bulk than predicted. Especially interesting is the lower part of Fig. 7 where the geometry is such that $q_z = 0$. In this case the modes are predicted to be degenerate at $d_1 = d_2$ which is borne out by the measurements where the mode separation becomes much smaller when approaching $d_1/d_2 = 1$, being unresolved at $d_1/d_2 = 1.35$.

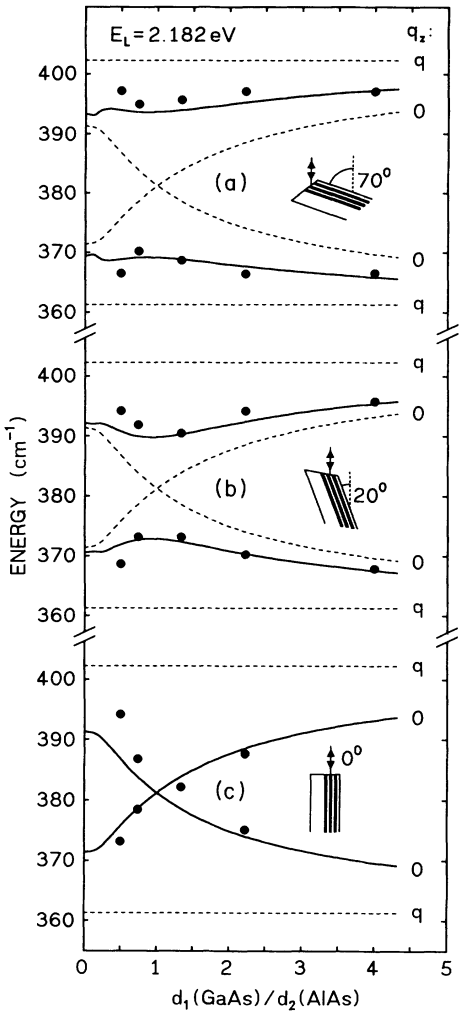

FIG. 7. Measured (dots) and calculated (solid lines) IF phonon energies as a function of d_1/d_2 for three different scattering geometries with increasing in-plane momentum transfer. The dashed lines are the calculated curves for $q_z = 0$ and $q_x = q$. A GaAs layer thickness $d_1 = 100$ Å was taken for the calculations.

IV. CONCLUSION

Using micro-Raman spectroscopy, we have studied the optical-phonon region of five GaAs/AlAs [001] superlattices. The submicrometer laser spot size allowed us to investigate several backscattering geometries—in particular, those with photon electric fields in the growth direction. The observed Raman intensities for the longitudinal and transverse confined optical modes could not be explained by the predictions of a recently developed microscopic theory.[14]

The IF phonon dispersion was then investigated over a wide range of in-plane momentum for each sample. This was realized by tilting the sample relative to the laser light and also varying the laser energy. Good agreement was found with the dielectric-continuum model and the IF phonon "gap" was preserved even for the largest in-plane momenta.

Finally, the AlAs IF phonon energy as a ratio of GaAs and AlAs thickness was studied where characteristic minima of the mode separation at equal thicknesses were observed. Again, the dielectric-continuum model agreed well with our results.

These studies of the IF phonons clearly demonstrate that momentum is conserved for the scattering process observed in our experiments. Therefore, impurity-induced scattering or symmetry-breaking resonance effects cannot be contributing significantly to the observed anomalous confined optical phonon cross sections.

ACKNOWLEDGMENTS

This work was supported financially by the Deutsche Forschungsgemeinschaft. One of us (M.H.) would also like to thank the Royal Society of London for support.

*Present address: Lehrstuhl für Experimentalphysik IV, Universität Augsburg, Memminger Str. 6, 8900 Augsburg, Germany.

†Present address: Sektion Physik, Universität München, Geschwister Scholl Platz 1, 8000 München 22, Germany.

[1]R. Merlin, C. Colvard, M. V. Klein, H. Morkoç, A. Y. Cho, and A. C. Gossard, Appl. Phys. Lett. **36**, 43 (1980).

[2]M. V. Klein, IEEE J. Quantum Electron. **QE-22**, 1760 (1986).

[3]B. Jusserand and M. Cardona, in *Light Scattering in Solids,* edited by M. Cardona and G. Güntherodt (Springer, Berlin, 1989), Vol. 5.

[4]M. Cardona, Superlatt. Microstruct. **5**, 27 (1989).

[5]J. Menéndez, J. Lumin. **44**, 285 (1989).

[6]R. Enderlein, D. Suisky, and J. Röseler, Phys. Status Solidi B **165**, 9 (1991).

[7]A. K. Sood, J. Menéndez, M. Cardona, and K. Ploog, Phys. Rev. Lett. **54**, 2111 (1985).

[8]G. Fasol, M. Tanaka, H. Sakaki, and. Y. Horikoshi, Phys. Rev. B **38**, 6056 (1988).

[9]D. J. Mowbray, M. Cardona, and K. Ploog, Phys. Rev. B **43**, 1598 (1991).

[10]D. Strauch and B. Dorner, J. Phys. Condens. Matter **2**, 1457 (1990).

[11]S. Baroni, P. Giannozzi, and E. Molinari, Phys. Rev. B **41**, 3870 (1990).

[12]P. Giannozzi, S. de Gironcoli, P. Pavane, and S. Baroni, Phys. Rev. B **43**, 7231 (1991).

[13]J. E. Zucker, A. Pinczuk, D. S. Chemla, A. Gossard, and W. Wiegmann, Phys. Rev. Lett. **53**, 1280 (1984).

[14]K. Huang, B. Zhu, and H. Tang, Phys. Rev. B **41**, 5825 (1990).

[15]A. K. Sood, J. Menéndez, M. Cardona, and K. Ploog, Phys. Rev. Lett. **54**, 2115 (1985).

[16]M. Nakayama, M. Ishida, and N. Samo, Phys. Rev. B **38**, 6348 (1988).

[17]A. Huber, T. Egeler, W. Ettmüller, H. Rothfritz, G. Tränkle, and G. Abstreiter, Superlatt. Microstruct. **9**, 309 (1991).

[18]E. D. Palik, in *Handbook of Optical Constants of Solids,* edited by E. D. Palik (Academic, Orlando, 1985).

[19]S. Adachi, J. Appl. Phys. **58**, R1 (1985).

[20]M. Cardona, in *Light Scattering in Solids,* edited by M. Cardona and G. Güntherodt (Springer, Berlin, 1983), Vol. II.

[21]R. E. Camley and D. L. Mills, Phys. Rev. B **29**, 1695 (1984).

[22]*Physics of Group IV Elements and III-V Compounds,* edited by O. Madelung, Landolt-Börnstein, New Series, Group 3, Vol. 17a (Springer, Berlin, 1982).